JOURNAL OF Applied Polymer SCIENCE

Toughening of poly(L-lactide) modified by a small amount of acrylonitrile–butadiene–styrene core-shell copolymer

Ningjing Wu, Hong Zhang
Key Laboratory of Rubber-Plastics, Ministry of Education/Shandong Provincial Key Laboratory of Rubber-Plastics, Qingdao University of Science & Technology, Qingdao City 266042, People's Republic of China
Correspondence to: N. Wu (E-mail: ningjing_wu@qust.edu.cn or ningjing_20132013@163.com)

ABSTRACT: A small amount of acrylonitrile-butadiene-styrene (ABS) core shell copolymer particles are used to improve the toughness of poly(L-lactide) (PLLA) matrix. The incorporation of ABS copolymer dramatically increased the elongation yield at break of PLLA. For PLLA blend with 6.0 wt % ABS copolymer particles, the elongation yield at break increased by 28 times and the notched impact strength improved by 100% comparing with those of neat PLLA. Fourier transformed infrared (FTIR) and dynamic mechanical analysis (DMA) and scanning electron microscopy (SEM) measurement results indicated that the special polarity interaction between ester group of PLLA matrix and nitrile group of PSAN shell phase enhanced the interfacial adhesion between PB rubber phase and PLLA matrix and promoted the fine dispersion of ABS particles in PLLA matrix. Meanwhile, ABS core shell particles also showed a certain extent of effects on the crystallinity behavior of PLLA. A small amount of ABS particles became the nucleating sites, and then the degree of crystallinity of PLLA/ABS blends increased. However, the notched impact of PLLA blends decreased because of the aggregation of more ABS particles. © 2015 Wiley Periodicals, Inc. J. Appl. Polym. Sci. **2015**, *132*, 42554.

KEYWORDS: biopolymers and renewable polymers; blends; mechanical properties; morphology

Received 11 December 2014; accepted 27 May 2015
DOI: 10.1002/app.42554

INTRODUCTION

The core-shell copolymer is very effective toughening agent for polymer, its core is "locked in" by slight crosslinking and grafting with its shell to keep them the physical combination with polymer matrix during mechanical blending.[1,2] The interaction between core-shell polymer and polymer matrix strongly depends on the miscibility of the shell layer of the core shell polymer with the polymer matrix. In general, the partial miscibility of the shell layer and polymer matrix is used to obtain polymer blends of desired modified impact properties.[3,4] For example, Methyl methacrylate-butadiene-styrene (MBS) and Acylic Rubber (ACR) are generally used as very effective impact modifiers for Polyvinyl chloride (PVC). Poly (butadiene) (PB) or poly(butyl acrylate) rubbery phase at inner core is the dominant toughening agent and Poly(methyl methacrylate) (PMMA) shell phase effectively enhances the interfacial adhesion between the PB rubber and PVC matrix.[5] The impact strength of PVC modified by less than 10 wt % MBS was dramatically improved about 10 times than that of PVC.[6]

Poly(L-lactic acid) (PLLA) is biodegradable and biocompatible semicrystalline polymer with high strength and high modulus that can be produced from renewable sources. It is a promising biomaterial for biomedical applications such as implant materials and drug delivery systems.[7–12] However, major disadvantages of PLLA including its inherent brittleness and low heat deflection temperature and low crystallization rate restricted its large-scale commercial applications. Numerous investigations have been carried out to modify the mechanical properties and crystallization behaviors of PLLA. PLLA has been blended with various biodegradable or nonbiodegradable polymers such as poly(ε-caprolactone) (PCL),[14] poly(ethylene glycol) (PEG),[15] poly(hydroxyl butyrate) (PHB),[16] Polybutylene succinate (PBS),[17] Polycarbonate (PC),[18] Polyethylene (PE),[19] Polyurethane (PU),[20] hyperbranched polymers,[9] polyamide resin,[21,22] thermoplastic polyolefin elastomer,[23,24] rubbers[25] to enhance its toughness properties. In order to achieve the desired mechanical properties of materials, most of the investigations are focused on the polymer blending by addition of a large amount of modifier with excess 10 wt % or even 20 wt %, the improvement of the fracture toughness of these polymer blends inevitably accompanied by a significant drop of the modulus and tensile strength.[26–31] The mechanical properties of PLLA have been ever modified by 5–25 wt % MBS core shell copolymers.[32] We investigated the mechanical properties of PLLA modified by ACR core shell copolymer nanoparticles in previous study.[33] The results showed that PLLA with a small amount

© 2015 Wiley Periodicals, Inc.

of modifier could achieve the enhancement of desired mechanical properties because the modifiers in the matrix formed very fine dispersions.[32–34]

ABS core shell copolymer is synthesized by PB seed emulsion polymerization of styrene and acrylonitrile monomer solution, which is very good toughening modifier for ABS resin to efficiently improve the interfacial interaction between PB rubber phase and ABS resin matrix.[12] The polarity of PSAN shell layer could be adjusted by controlling the composition of polystyrene and polyacrylonitrile. It is quite reasonable to expect that the incorporation of ABS core shell copolymer particles into PLLA may bring about improved toughness of PLLA. Because ABS core shell copolymer is an industrial and mass-produced and inexpensive modifier, it is very valuable and meaningful to promote large-scale application of modified PLLA in the engineering plastic field. In this article, the mechanical properties and crystallization behaviors of PLLA blend modified by a small amount of ABS core shell particles are systematically studied, and the miscibility of and phase morphology of PLLA/ABS blends have been investigated by dynamic mechanical analysis (DMA), FTIR, and SEM measurements.

EXPERIMENTAL

Materials

PLLA pellets (Natureworks 2003D, $M_w = 38 \times 10^4$g mol^{-1}, $M_w/M_n = 1.59$) were purchased from American Natureworks Company. ABS core shell copolymer particles ($M_w = 30 \times 10^4$g mol^{-1}) were prepared by emulsion polymerization in lab.

Preparation of Samples

The weight ratio of PB core layer and PSAN shell layer is 60/40 (w/w). The average size of ABS particles is about 100−200 nm, and the thickness of the outer shell PSAN layer is about 20−30 nm by TEM measurement.

PLLA blend samples with different content of ABS core shell particles were melt-mixed using Hakke polylab OS (Thermo Fisher Scientific, Germany) at 190°C for 8 min with a rotor speed of 50 rpm. After blending, the samples were hot-pressed at 200°C for 5 min under the pressure of 10 MPa into sheet with different thickness of 1 mm and 4 mm, respectively, and followed by quickly cooling at the room temperature. The tensile and impact samples were prepared by cutting standard size.

Characterization of Samples

Scanning Electron Microscopy (SEM) and Transmission Electron Microscopy (TEM) were used to observe the morphology of the PLLA/ABS blend samples. The samples were fractured to obtain the random fracture surface after immersion in liquid nitrogen for 10 min. The fracture surfaces were uniformly coated with a thin layer of gold. Scanning electron microscope (SEM 7500F JEOL, Japan) was used to observe both the morphology of PLLA/ABS blend and ABS particles distribution in the fracture of the PLLA/ABS blend films at an acceleration voltage of 10 kV.

PLLA/ABS blend samples were ultramicrotomed at −120°C to a section with a thickness of 70 nm. The section was stained with ruthenium tetroxide (RuO4) for 20 min. The PLLA/ABS blend sample was observed by TEM (2010HR, Japan Electron Company) with an acceleration voltage of 75 kV.

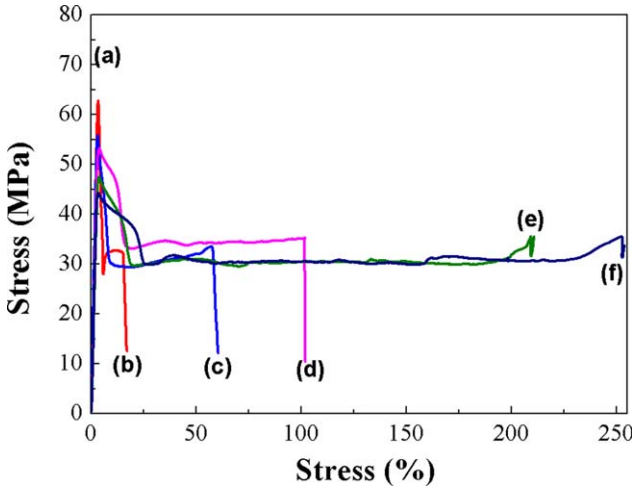

Figure 1. Stress−strain curves for PLLA and PLLA/ABS blend films. (a) neat PLLA (b) PLLA/2 wt % ABS (c) PLLA/4 wt % ABS (d) PLLA/6 wt % ABS (e) PLLA/8 wt % ABS (f) PLLA/10 wt % ABS. [Color figure can be viewed in the online issue, which is available at wileyonlinelibrary.com.]

Differential Scanning Calorimetry (DSC) measurement was carried out under nitrogen flow at a heating rate of 10 K/min with a differential scanning calorimetry (DSC) system (TA Company Q-20). The films were first heated rapidly at rate of 50°C/min from room temperature to 180°C and followed by isothermal heating for 2 min in order to eliminate the heat history of samples, and then cooled to 0°C and second heated from 0°C to 180°C at a rate of 10°C/min in nitrogen atmosphere. It is normalized both enthalpies of fusion and crystallization, with respect the weight fraction of the crystalline component. The X_c% should be estimated from the normalized value of enthalpy of fusion.

Dynamic Mechanical Analysis (DMA) was carried out with a TA Instruments Model Q800 apparatus in the tensile mode. All the measurements were performed in the linear region. Storage modulus (E), loss modulus (E'), and dynamic loss tangent (tanδ) were determined with a function of temperature from 150°C to 150°C at a frequency of 1Hz and a heating rate of 3°C/min.

Fourier Transformed Infrared (FTIR) spectra were measured with a Bruker Tensor 27 spectrometer using transmission mode. The thin film sample was prepared by direct hot pressing of melt-blending sample at 190°C. The thickness is about 20−40 μm.

Mechanical Properties Measurements

Tensile measurements were performed on a screw-driven universal testing machine equipped with an electronic load cell and mechanical grips (AL-7000M, Taiwan Gotech Testing Machines). The extensometer size is 25KN. The tests were conducted at room temperature using a cross-head rate of 30 mm/min according to the ASTM D882 standard. At least five specimens were tested for each sample.

Table I. Mechanical Properties of PLA Blends Modified with Several Percent of ABS Core-Shell Copolymers

Sample	Tensile strength (MPa)	Tensile modulus (GPa)	Elongation yield at break (%)	Notched impact strength (kJ/m^2)
PLLA	67.6 ± 0.9	1.8 ± 0.1	4 ± 1	3.4 ± 0.6
PLLA/2%ABS	63.4 ± 1.8	1.7 ± 01	27 ± 13	4.1 ± 0.7
PLLA/4%ABS	56.6 ± 2.6	1.5 ± 0.1	87 ± 27	6.1 ± 0.6
PLLA/6%ABS	52.3 ± 2.0	1.4 ± 0.0	118 ± 21	6.7 ± 0.8
PLLA/8%ABS	45.4 ± 1.3	1.3 ± 0.1	225 ± 16	4.8 ± 0.5
PLLA/10%ABS	42.7 ± 0.1	1.1 ± 0.0	275 ± 20	5.8 ± 0.9

The izod impact tests were carried out according to GB/T1043.1–2008 using an impact tester (Suzhou Ligao Detection Equipment) on the standard sized rectangular bars at room temperature. At least five specimens were tested for each sample to get an average value.

RESULTS AND DISCUSSION

Mechanical Properties and Morphologies of PLLA/ABS Blends

Mechanical properties of the PLLA blends with different content of ABS core shell copolymer have been evaluated. The stress−strain curves of PLLA and PLLA blend films are shown in Figure 1. The elongation at break of the neat PLLA is only about 4.4%; and it is observed that the necking process occurs at larger strain for PLLA blend films with several percent ABS core-shell copolymers than that of neat PLLA, the elongation yield of PLLA blend films drastically increases with the addition of a small amount of ABS particles. Specially, for PLLA blend with 10 wt % ABS, the elongation at break of the blend achieves about 274.8%, which is about 62 times larger than that of the neat PLLA. The tensile properties and notched impact strength are presented in Table I. The notched impact strength for neat PLLA is 3.4 KJ/m^2. With the increasing of ABS core shell copolymer content, the notched impact strength increases. The tensile strength and the tensile modulus for PLLA blend film decrease with the increasing of ABS core shell copolymer content. When the ABS copolymer content is 6.0 wt %, the elongation yield at break and the impact strength of PLLA/ABS blend sample are increased to 118% and 6.7 KJ/m^2, respectively. The tensile strength and the tensile modulus for PLLA blend with 6 wt % ABS decrease to 52.3 MPa and 1.4 GPa, respectively. The mechanical properties results show that the elongation yield at break and impact strength of PLLA with several percents of ABS core-shell copolymer can be improved.

The impact fracture surface of PLLA/ABS blend films and the distribution of ABS particles in the PLLA matrix are shown in Figure 2. For neat PLLA sample in Figure 2(a), it presents smooth fracture structure, which indicates classical brittle plastic

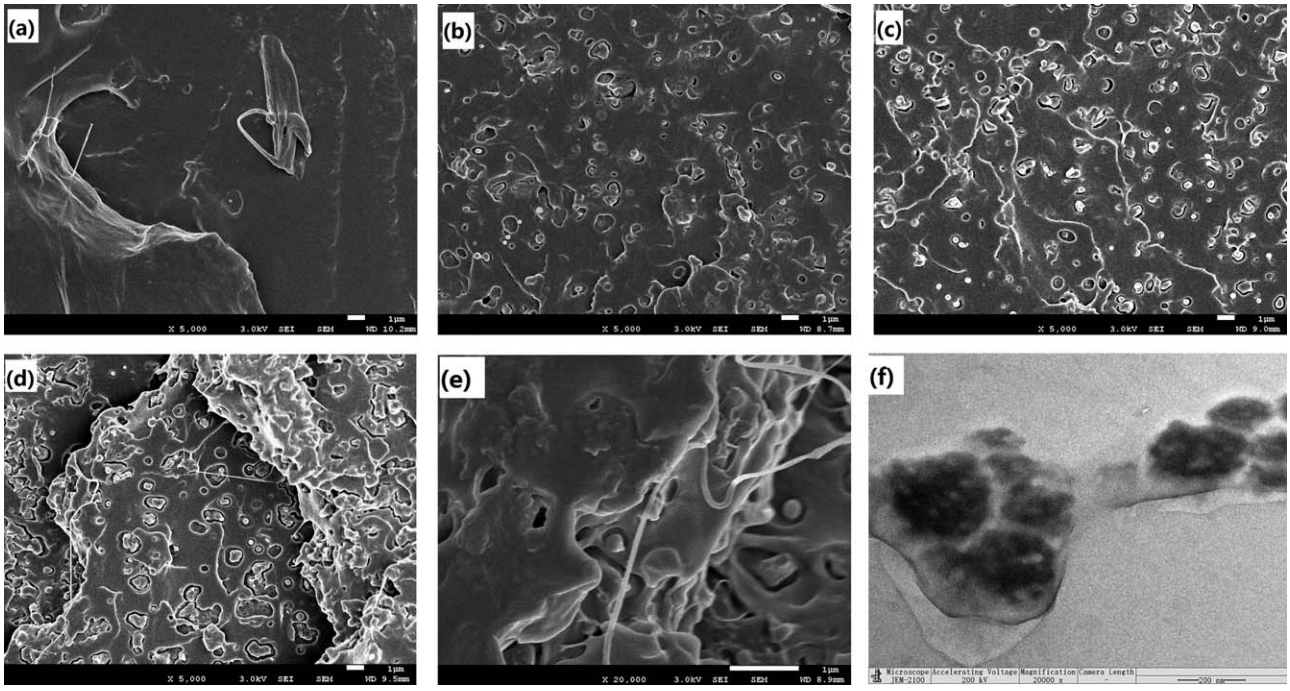

Figure 2. SEM images (a−e) and TEM image (f) of PLLA/ABS blends. (a) PLLA (b) PLLA/2 wt % ABS (c) PLLA/4 wt % ABS (d) PLLA/8 wt % ABS. (e) PLLA/10 wt % ABS (f) PLLA/10 wt % ABS.

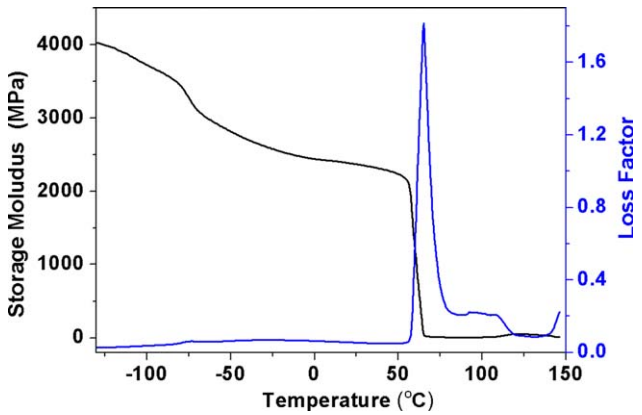

Figure 3. Dynamic curves of PLLA/10%ABS blend in the temperature range of °−140 to 140°C. [Color figure can be viewed in the online issue, which is available at wileyonlinelibrary.com.]

deformation. From Figure 2(b), the facture surface for PLLA/2 wt % ABS blend sample presents coarse phase structure, and ABS particles are relatively homogeneously dispersed in the PLLA matrix with the dimension from 100 to 300 nm, which form from nanoscale to microscale-dispersed phase structure in PLLA matrix. It is observed that ABS core shell copolymer particles are cavitated at the fracture in Figure 2(c). In general, the cavities are formed when the volumetric impact energy released by forming a void is greater than the surface energy needed to form new surface plus the energy needed to impact the surrounding rubber to make space for the void.[16,17] These cavitated ABS particles in submicrometer scale effectively dissipate impact energy. With the increasing of ABS core shell copolymer content, the large voids are formed by the aggregation of neighboring small particles. In addition, extensive plastic deformation of the PLLA matrix could be clearly observed in Figure 2(d), which implied that shear yielding of the PLLA matrix. Some fibrils could be also observed at the fracture surface of the PLLA/ABS blends, and the number of fibrils increased with the increasing of ABS content. Such fibril-like structures have been reported in other rubber modified polymers.[20–22] The phenomena are attributed that there are good interfacial interaction between ABS particles and PLLA matrix. Figure 2 shows the fracture and bulk morphologies comparison of PLLA/10%ABS blend sample. For SEM photograph of the PLLA/ABS blend samples in Figure 2(e), it presents not only some cavitations but also the fibrils and obvious matrix plastic deformation. This explains why is the tensile toughness of PLLA films improved by a small amount of ABS particles. However, it is also observed that ABS particles are aggregated with the dimension of 400−500 nm in Figure 2(f), which is one main reason why the impact strength cannot be further improved.

Dynamic Mechanical Analysis of PLLA/ABS Blends

Figure 3 demonstrates the storage modulus curves as a function of temperature for PLLA/ABS blend. PLLA phase has a high storage modulus (E) in the temperature region of −130 to 50°C. The E value of PLLA/ABS alloy drops abruptly at 50−60°C. The dynamic loss appears the maximum value at 65°C due to the glass transition of PLLA, and it rises with temperature rising due to the PLLA cold crystallization of PLLA.[34] From the dynamic loss modulus curves in Figure 4, it is observed that there exist the two glass-transitions for PLLA/ABS blends in Figure 4(a). The first transition temperature for PLLA with 8% ABS is about −75.3°C, which corresponds to the glass transition temperature (T_{g1}) of inner PB core phase. The second transition temperature is about 58.6°C, which is ascribed to the glass transition temperature (T_{g2}) of PLLA matrix. When the content of ABS core shell particles increases from 4% to 10%, T_{g1} values for PLLA/ABS blends slightly increase from −76.5 to −74.9°C. Meanwhile, T_{g2} values for the PLLA /ABS blends increase from 58.0°C to 59.0°C, shown in Figure 4(b). The DMA data of PLLA and PLLA/ABS blend are shown in Table II. The outer shell layer phase in ABS copolymer is constituted of Poly (styrene-acrylonitrile) random copolymer (PSAN) by free-radical emulsion polymerization. It is suggested that the improvement of T_{g2} of PLLA in the PLLA/ABS blend originates from the special interaction between the PLLA matrix and outer shell PSAN phase of ABS copolymer. The glass transition temperatures of PS (Polystyrene) and PAN (Polyacrylonitrile) are

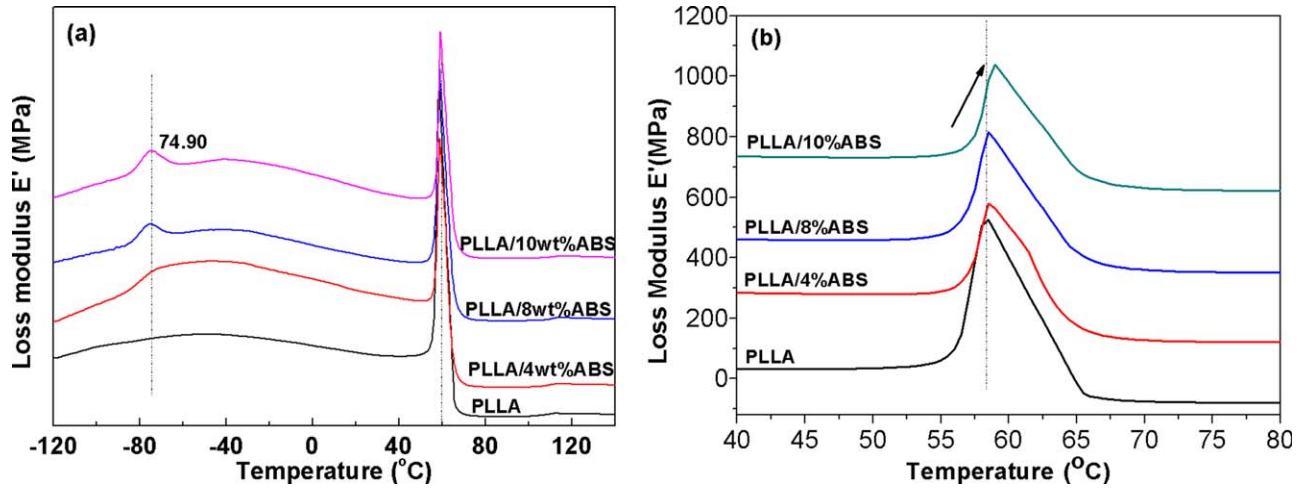

Figure 4. The loss modulus curves of PLLA and PLLA/ABS blends in the temperature range of (a) −120 to 120°C. (b) 40−80°C. [Color figure can be viewed in the online issue, which is available at wileyonlinelibrary.com.]

Table II. The Glass Transition Temperature Data of PLLA and PLLA/ABS Blend Samples by DMA Measurement

Samples	T_{g1} (°C)	T_{g2} (°C)
PLLA	–	58.0
PLLA/4% ABS	−76.5	58.4
PLLA/8%ABS	−75.3	58.6
PLLA/10%ABS	−74.9	59.0

about 100°C and 85°C, respectively, but it is not observed the T_g of PS or PAN phase in the enlarged DMA curve due to the low PSAN content in PLLA/ABS blends and the random copolymer structure of PSAN copolymer. In order to confirm the suggestion, FTIR spectra of PLLA and PLLA blend film samples are further measured.

FTIR Spectra of PLLA and PLLA/ABS Blends

The FTIR spectra for PLLA and PLLA blends with the different content of ABS copolymer in the range of 2000−800 cm^{-1} are shown in Figure 5 (a). The characteristic peaks at 1758 and 1090 cm^{-1} are corresponding to the vibration absorptions of carbonyl group (C═O) and ester group (C—O) of PLLA, respectively.[35] With the incorporation of ABS core shell copolymer, it is observed that that the carbonyl group and ester group characteristic peaks are obviously split more than two peaks. From the enlarged FTIR spectra of PLLA/ABS blend in Figure 5 (b), the new peaks at 1100 cm^{-1} and 1088 cm^{-1} become more obvious and the peak intensities become stronger with the increasing of ABS core shell copolymer content. Meanwhile, the characteristic peak at 1758 cm^{-1} is also split into the new peaks at 1765, 1762, and 1752 cm^{-1} with the addition of ABS core shell particles in Figure 5(c), and the new peak intensities become stronger with the increasing of ABS copolymer content. Table III lists the characteristic band assignments of amorphous and semi-crystalline PLLA thin film in the range of 1800−1000 cm^{-1}. The new peaks at 1088 cm^{-1} and 1762 cm^{-1} are ascribed to the crystalline peak of PLLA. It means that the crystalline behavior of PLLA changes with the addition of ABS core copolymer. Why do the other new characteristic peaks in carbonyl group and ester group split? Because PSAN shell layer for ABS particles locates at the interface between the PB rubber core phase and PLLA matrix, it is speculated that the strong polarity interaction between nitrile group of PSAN chains in

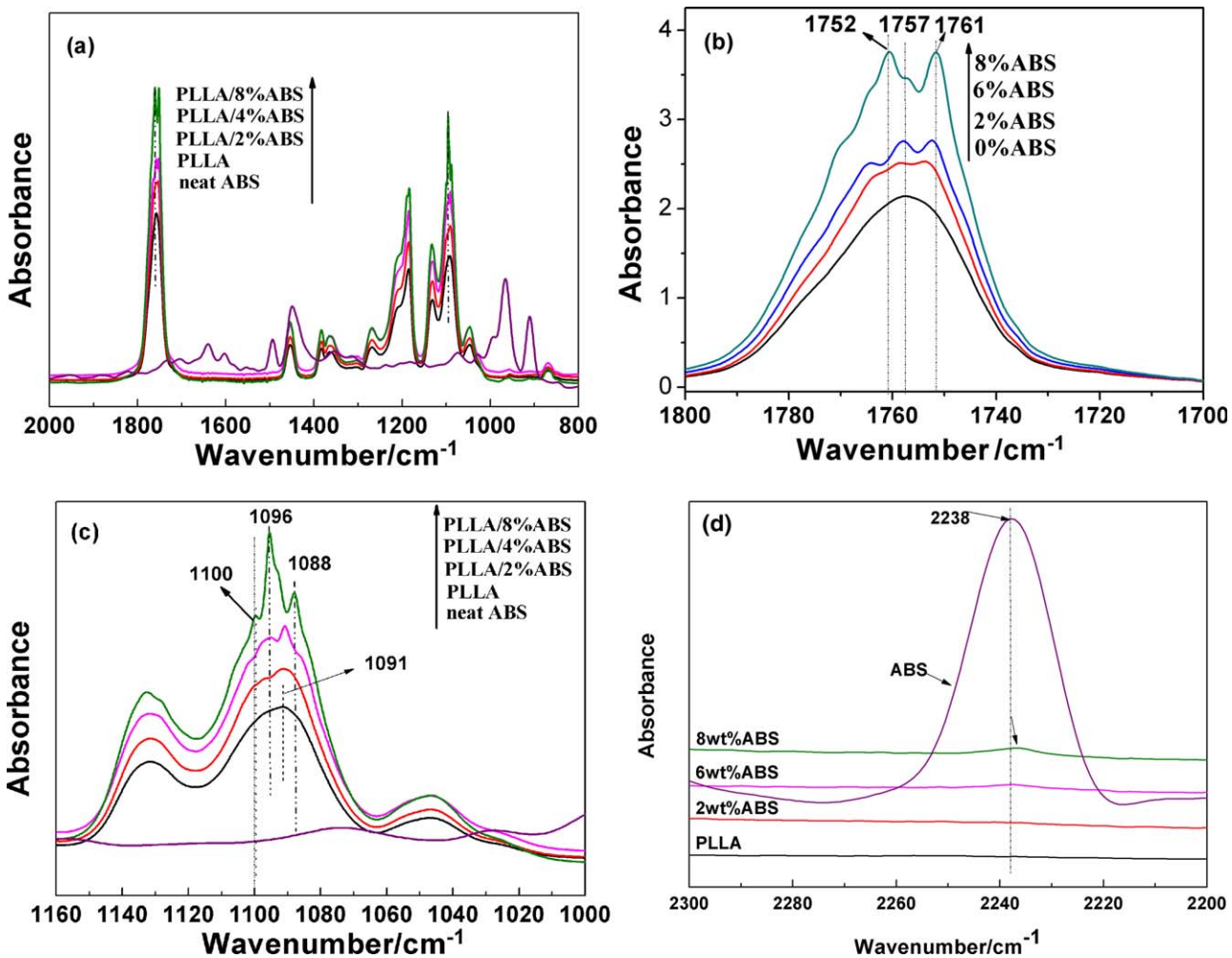

Figure 5. FTIR spectra of PLLA and PLLA/ABS blend and ABS copolymer films in the range of 2000−800 cm^{-1} (a), 1800−1700 cm^{-1} (b), 1160−1000 cm^{-1} (c), 2300−2200 cm^{-1} (d). [Color figure can be viewed in the online issue, which is available at wileyonlinelibrary.com.]

Table III. Infrared Band Characteristic Assignments of Amorphous and Semicrystalline PLLA Ultrathin Film in the Range of 1800−1000 cm^{-1}

IR frequencies (cm^{-1})			
	Semicrystalline		
Amorphous	α′	α	Assignments
1757	1762	1759	ν (C=O)
		1749	
1454	1458	1458	$\delta_{as}(CH_3)$
		1444	
1383	1386	1386	$\delta_s(CH_3)$
		1382	
1363	1368	1368	δ(CH), CH wagging
		1360	
1268	1268	1268	ν (CH)+ ν (COC)
1212	1215	1215	ν_{as}(COC)+ r_{as} (CH_3)
1182	1184	1184	ν_{as} (COC)+r_{as} (CH_3)
	1194	1194	
1089	1107	1107	ν_s(COC)
	1089	1089	

shell layer and ester group of PLLA induce the characteristic peak of C=O and C—O groups to shift and divide into other new peaks, and the branching trend of the characteristic peak of PLLA becomes greater with the increasing of ABS copolymer content. From the enlarged spectra in Figure 5(d), it is observed that the characteristic peak at 2348 cm^{-1} of the nitrile group of neat ABS slightly shifts to lower peak at 2346 cm^{-1} of the nitrile group of PLLA/8 wt % blend, which also proves the polarity interaction between the nitrile groups of PSAN shell and the carbonyl group of PLLA. The polarity interaction of ABS and PLLA enhances the interfacial adhesion of ABS particles and PLLA matrix.

Crystallization Behavior of PLLA/ABS Blends

Based on the above FTIR measurement, it indicates that the crystalline behavior of PLLA changes with the addition of ABS core copolymer. Figure 6 shows the DSC heating and cooling curves at a rate of 10°C/ min for the neat PLLA and PLLA/ABS blends. Figure 6(a) exhibits three main transitions of PLLA phase: a glass transition, a cold crystallization exotherm, and a melting endotherm. Very minor crystallization peak is observed for the neat PLLA, indicating PLLA is difficult to crystallize at heating rate of 10°C/min. When the ABS copolymer content is 2.0 wt %, the cold crystallization start temperature (T_{cs}) of PLLA/ABS blend is lower than that of neat PLLA, and the crystallization degree (X_c) of PLLA/ABS blend is higher than that of neat of PLLA, which indicates that a small amount of ABS particles are acted as nucleation agent on the cold crystallization process of PLLA. However, with the increasing of ABS content, the cold crystallization start temperature (T_{cs}) of the PLLA blend is close to or even higher than that of neat PLLA, it is because more ABS particles hinder the crystal growth and reduce the crystallization rate of PLLA in the PLLA/ABS blends. Therefore, the melt crystallization enthalpy and the degree of crystallization (X_c) for PLLA/ABS blends decrease with the increasing of ABS content in Table IV. The DSC cooling curves of PLLA blends are shown in Figure 6(d), it is observed the crystallinity degrees of PLLA and PLLA/ABS blend obtained from cooling curve at 10°C/min are very close to zero. In our previous study, the crystallinity degree of PLLA obtained from heating curve is very low.[33] Therefore, the incorporation of ABS particles cannot promote the melt crystallization of PLLA.

CONCLUSIONS

Toughing of semicrystalline polymers by blending with elastomers has been extensively reported;[14−24] the improvement of toughness of these polymer blends by the addition of a large amount of elastomer modifier is inevitably accompanied by a significant drop in the modulus and tensile strength. In order to improve the compatibility of PLLA matrix and elastomer modifier, a small amount of ABS core shell copolymer particles are used to modify the toughness of PLLA matrix in this article, it is investigated that a small amount of ABS core shell particles in PLLA matrix show markedly increased elongation yield at

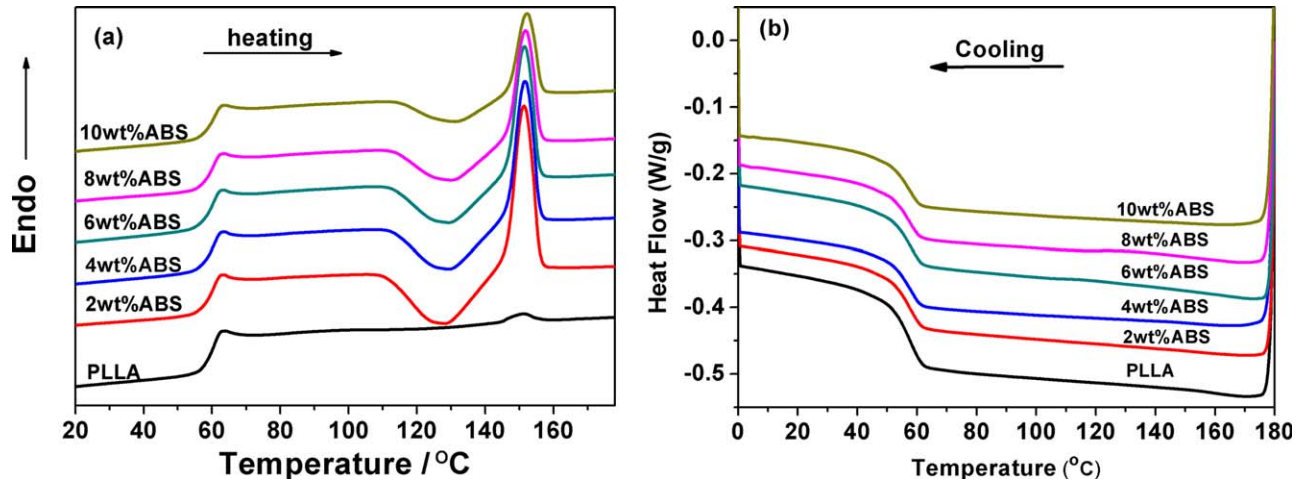

Figure 6. DSC curves of PLLA and PLLA/ABS blends at 10°C/min. (a) heating from 0 to 180°C, (b) cooling from 180 to 0°C. [Color figure can be viewed in the online issue, which is available at wileyonlinelibrary.com.]

Table IV. Thermal Properties of PLLA and PLLA/ABS Blend Film by DSC Measurement

Samples	T_g (°C)	T_{cs} (°C)	T_{cm} (°C)	T_{ce} (°C)	T_m (°C)	ΔH_f (J/g)	X_c (%)
PLLA	60.9	112.5	129.2	143.9	151.3	0.5	0.6
PLLA/2%ABS	59.8	110.3	126.5	142.3	150.9	18.4	20.2
PLLA/4%ABS	61.1	113.7	130.1	144.1	152.2	15.1	16.9
PLLA/6%ABS	60.4	112.5	129.6	145.7	151.5	14.3	16.4
PLLA/8%ABS	61.0	115.1	132.1	146.5	152.3	11.8	13.8
PLLA/10%ABS	60.6	115.4	132.2	146.0	152.5	7.2	8.6

The melt enthalpy of neat PLLA (ΔH : 93 J/g) X_c, crystallinity degree of PLLA.

break and improved impact strength as well. The elongation yield at break of PLLA sample with 6.0 wt % ABS core shell copolymer particles increases by 28 times and the notched impact strength improves by 100% comparing with those of neat PLLA. With the increasing of ABS content, the elongation yield of PLLA/10 wt %ABS blend achieves about 274.8%; however, the impact strength of PLLA blend decreases because the dispersion of ABS core shell copolymer particles into PLLA matrix becomes worse. For ABS core shell particle, PB rubber is used as inner core layer and acrylonitrile-styrene random copolymer is used as outer shell layer. We attribute the toughing effects to several factors induced by the ABS particles. On the one hand, it is observed by SEM measurement that ABS core shell copolymer particles are cavitated in PLLA matrix and some fibrils are formed in the impact, and then PB rubber phase effectively absorbs the massive impact energy. On the other hand, the DMA and FTIR measurement results show that it presents special polarity interaction between ester group of PLLA matrix and nitrile group of PSAN shell phase in ABS core shell copolymer, and then PSAN shell phase of ABS particles could effectively enhance the interfacial adhesion between the PB rubber phase and PLLA matrix, which results in the partial compatibility of PLLA and ABS core shell copolymer. Meanwhile, ABS core shell particles also show a certain extent of effects on the crystallinity behavior of PLLA. A small amount of ABS particles become the nucleating sites, and then the degree of crystallinity of PLLA/ABS blend increases. With the content of the ABS core shell particles content is 10 wt %, ABS particles of diameter above 400 nm could be aggregated in PLLA matrix, which causes nonuniform distribution of ABS particles in PLLA matrix, and then the notched impact of PLLA/ABS blends decrease.

ACKNOWLEDGMENTS

It is grateful for the financial supports from Natural Science Foundation of China (21104038).

REFERENCES

1. Lovell, P. A.; Mcdonald, J.; Saunders, D. E. J.; Young, R. J. *Polymer* **1993**, *34*, 61.
2. Kolarlk, J.; Lednicky, F. *Polym. Eng. Sci.* **1992**, *32*, 886.
3. Si, Q. B.; Zhou, C.; Yang, H. D.; Zhang, H. X. *Eur. Polym. J.* **2007**, *43*, 3060.
4. Crawford, E.; Lesser, A. J. *Polymer* **2000**, *41*, 5865.
5. Havriliak, S. J.; Slavin, S. E.; Shortridge, T. *J. Polym Int.* **1991**, *25*, 67.
6. Havriliak, S. J.; Shortridge, T. J. *J. Polym. Sci. Part B: Polym. Phys.* **1990**, *28*, 1987.
7. Gross, R. A.; Kalra, B. *Science* **2002**, *297*, 803.
8. Hu, Y.; Sato, H.; Zhang, J. M.; Noda, I.; Ozaki, Y. *Polymer* **2008**, *49*, 4204.
9. Bhardwaj, R.; Mohanty, A. K. *Biomacromolecules* **2007**, *8*, 2476.
10. Park, J. W.; Im, S. S. *J. Appl. Polym. Sci.* **2002**, *86*, 647.
11. Zhang, G. B.; Zhang, J. M.; Wang, S. G.; Shen, D. Y. *J Polym. Sci. Part B: Polym. Phys.* **2003**, *41*, 23.
12. Kelly, S. A.; Kathleen, M. S.; Marc, A. H. *Polym. Rev.* **2008**, *48*, 85.
13. Liu, H. Z.; Zhang, J. W. *J. Polym. Sci. Part B: Polym. Phys.* **2011**, *49*, 1051.
14. Na, Y. H.; He, Y.; Shuai, X. T.; Kikkawa, Y.; Inoue, Y. *Biomacromolecules* **2002**, *3*, 1179.
15. Kulinski, Z.; Piorkowska, E. *Polymer* **2005**, *46*, 10290.
16. Focarete, M. L.; Scanodola, M.; Dobrzynski, P.; Kowalczuk, M. *Macromolecules* **2002**, *35*, 8472.
17. Wang, R. Y.; Wang, S. F.; Zhang, Y.; Wan, C. Y.; Ma, P. M. *Polym. Eng. Sci.* **2009**, *49*, 26.
18. Wang, Y. H.; Shi, Y. Y.; Dai, J.; Yang, J. H.; Huang, T.; Zhang, N.; Peng, Y.; Wang, Y. *Polym. Int.* **2013**, *62*, 957.
19. Singh, G.; Bhunia, H.; Rajor, A.; Jana, R. N.; Choudhary, V. *J. Appl. Polym. Sci.* **2010**, *118*, 496.
20. Feng, L. D.; Bian, X. C.; Cui, Y.; Chen, Z. M.; Li, G.; Chen, X. S. *Macromol. Chem. Phys.* **2013**, *214*, 824.
21. Zhang, W.; Chen, L.; Zhang, Y. *Polymer* **2009**, *50*, 1311.
22. Dong, W. Y.; Gao, X. J.; Li, Y. J. *Polym. Int.* **2014**, *63*, 1094.
23. Ho, C. H.; Wang, C. H.; Lin, C. I.; Lee, Y. D. *Polymer* **2008**, *49*, 3902.
24. Oyama, H. *Polymer* **2009**, *50*, 747.
25. Jaratrotkamjorn, R.; Khaokong, C.; Tanrattanakul, V. *J. Appl. Polym. Sci.* **2012**, *124*, 5027.
26. Zhang, C. M.; Man, C. Z.; Pan, Y. H.; Wang, W. W.; Jiang, L.; Dan, Y. *Polym. Int.* **2011**, *60*, 1548.
27. Hideko, T. O. *Polymer* **2009**, *50*, 747.

28. Kazuhiro, H.; Shotaro, N.; Takashi, I. *Polymer* **2012**, *51*, 3934.
29. Li, Y.; Iwakura, Y.; Zhao, L.; Shimizu, H. *Macromolecules* **2008**, *41*, 3120.
30. Anderson, K. S.; Hillmyer, M. A. *Polymer* **2006**, *47*, 2030.
31. Liu, H. Z.; Zhang, J. W. *J. Polym. Sci. Part B: Polym. Phys.* **2011**, *49*, 1051.
32. Zhang, H. L.; Liu, N. N.; Ran, X. H.; Han, C. Y.; Han, L. J.; Zhuang, Y. G.; Dong, L. S. *J. Appl. Polym. Sci.* **2012**, *125*, 550.
33. Wu, N. J.; Ding, M. C.; Zhang, J. M.; Lin, R. X. *Mater. Lett.* **2012**, *83*, 148.
34. Dong, W. Y.; Jiang, F. H.; Zhao, L. P.; You, J. C.; Cao, X. J.; Li, Y. J. *ACS Appl. Mater. Interfaces* **2012**, *4*, 3667.